Communications In Catalysis
Vol. 2, No. 2, 2025, pp. 44-55
Azarbaijan Shahid Madani University

One- pot facile synthesis of nitrogen doped graphene quantum dots based on N',2-dihydroxyethanimidamide and citric acid

Ebrahim Rezaii[1]*, Mehrdad Mahkam[2], Mohammad Rezaii[3]

[1,2]Chemistry Department, Faculty of Science, Azarbaijan Shahid Madani University, Tabriz, Iran

[3]Educational Sciences Department, Faculty of Science, Farhangian University, Tabriz, Iran

E-mail: Ebrahimrezayii@gmail.com

Received: 2025-10-14, Accepted: 2025-11-18

Abstract

Graphene quantum dots (GQDs) are tiny segments of graphene whose electron mobility is confined in all three dimensions. Graphene is a 0-bandgap semiconductor possessing an infinite exciton Bohr diameter. Therefore, quantum confinement is evident in all graphene fragments. The GQDs are usually under 20 nm in dimensions. We report a facile hydrothermal method for synthesis of graphene quantum dots contains nitrogen atoms (N-GQDs). This study shows interaction between citric acid (CA) and N',2-dihydroxyethanimidamide (DHAA) in which N-doped graphene quantum dots were synthesized. Due to use of DHAA that has two active sites, synthesized N-GQDs have special morphology, fluorescence and viscosity. Compared with other nitrogen compounds that is necessary for N-GQDs synthesis, DHAA is much more suitable due to low toxicity and stability. Synthesized N-GQDs were identified by FT-IR, XRD, TGA and fluorescence.

Keywords: N',2-dihydroxyethanimidamide, Nitrogen doped, Graphene quantum dot, One- pot synthesis

Introduction

graphene quantum dots (GQDs) that consist of nanometer-scaled graphene particles with sp^2-sp^2 carbon bonds are expected to show specific properties like size dependent general quantum dots (QDs) [1, 2] or chemically modified quantum dots with sp^2-sp^2 carbon bonds. In contrast to graphene, most applications of GQDs have been focused on the photoluminescence (PL)-related fields since GQDs show a PL. Recent studies clear that, additional properties of GQDs such as high transparency and high surface area have been discussed for energy and display applications [3].

Carbon quantum dots (C-QDs), have received many attentions for exceptional advantages such as low toxicity [4, 5], high chemical stability [6], excellent biocompatibility [7-9], high-fluorescence [10]. Considering these unique physical-chemical characteristics, C-QDs have been applied broadly in fields of catalysis [11], printing ink [12], biological sensors [13-15], bioimaging [16] and drug delivery [17]. Since 2006, Sun et al. found a new fluorescent nanoparticle named as carbon dots, many approaches have been found to prepare C-QDs [18]. Up to now, several methods for obtaining carbon-based materials have been developed, such as chemical oxidation method [19], ultrasonic method [20], hydrothermal synthesis [9, 21-23], solvothermal method [24], microwave method [25] and laser ablation method [18].

There are two main strategies for synthesizing GQDs, i.e., top-down and bottom-up methods. The first approaches involve the exfoliation of graphite into graphene sheets, followed by cutting of graphene sheets into GQDs. Therefore, the top- down method is limited by low product yield and rough conditions because of the use of a toxic organic solvent and strong acid/oxidant [26-28]. However, the bottom-up approaches is based on the construction of GQD from small organic precursor molecules through catalytic or thermal treatment, resulting in the environmentally-friendly production of large scale GQDs with uniform size of distribution and morphology [29, 30].

N-doped into graphene was highly effective in modulating its band gap to achieve new properties for device

applications [31, 32]. Due to the considerable quantum confinement and edge effects of GQDs, direct substitution with nitrogen in GQDs lattice can drastically modulate the chemical and electronic properties and offer more active sites, thus leading to unexpected phenomena which could be extensively applied in various fields. Recently, N-doped GQDs (N-GQDs) have been synthesized through hydrothermal or electrochemical methods which are based on slicing graphene oxide (GO) and its reduction. However, synthesis of GO typically takes several days and requires lots of strong chemical acid and oxidant in a series of chemical treatments of the bulk graphite powder [33, 34].

Chemical doping is one of the important and basic factors in improving the properties of graphene, which has been proved effective in the doping of carbon nanotubes (CNTs) and has extremely broadened their applications [35-39]. When a nitrogen atom is doped into graphene, three common bonding configurations within the carbon lattice, including quaternary N (or graphitic N), pyridinic N, and pyrrolic N are obtained (Figure 1) [40].

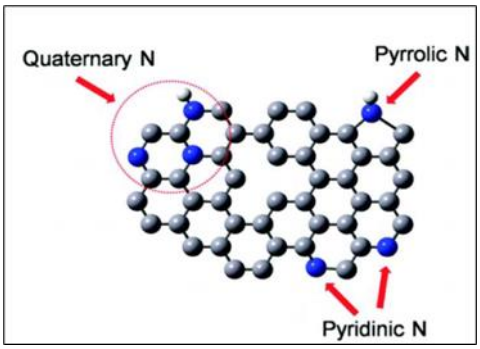

Figure 1: Three common bonding configuration nitrogen-doped graphene

Experimental

Materials

Citric acid and N',2-dihydroxyethanimidamide were purchased from Sigma Aldrich by purity of 99% and NaOH was purchased from Beijing Chemical Works and used directly without further purification.

Synthesis of N-GQDs

The N-GQDs were synthesized by carbonization of citric acid with N',2-dihydroxyethanimidamide through hydrothermal treatment. In brief, CA

and DHAA with different molar ratio (1:0.3, 1:1, 1:1.5, 1:3) were transferred to reaction vessel and heated at 170^{o}C using a heating mantle for 3h under open system. Subsequently, the color of the liquid was changed from colorless to pale yellow, and then orange in 1h, implying the formation of GQDs. Then cooled down to room temperature. After cooling, a suspension of N-GQDs were obtained. If the heating was kept on, the orange liquid would finally turn to black solid in about more than 3h, exits from QDs state.

Characterization

Powder X-ray diffraction (XRD) patterns of the samples were obtained with a Bruker D8 Advance diffractometer using a Cu Kα source (λ= 0.154056 nm). The FT-IR spectra were recorded on a Shimadzu FT-IR-408 spectrophotometer. Fluorescence spectra and intensity measurements were carried out using an FP-6200 spectrofluorometer (JASCO Corporation, Tokyo, Japan). The Thermogravimetric analysis (TGA) of the samples was measured using Mettler Toledo instrument under N_2 with a heating rate of 10 °C min^{-1}.

Result and Discussion

Effectiveness of the N atoms doping of GQDs was evaluated with FT-IR spectra, XRD, TGA and fluorescence.

FT-IR analysis

The Fourier transform infrared (FT-IR) spectra were measured to verify the functional groups. Figure 2 shows the FT-IR spectrums of N-GQDs with various DHAA contents. The spectrum of products was the same, showing a strong OH peak at 3443 cm^{-1}. The peaks related to N-C=O (1633 cm^{-1}) and C=C-H (1361 cm^{-1}) are also clearly observed. Bending peak at 666 cm^{-1} exhibits C-H, N-H. These results confirm the successful introduction of N in N-GQDs and are also consistent with the corresponding FT-IR spectroscopy results.

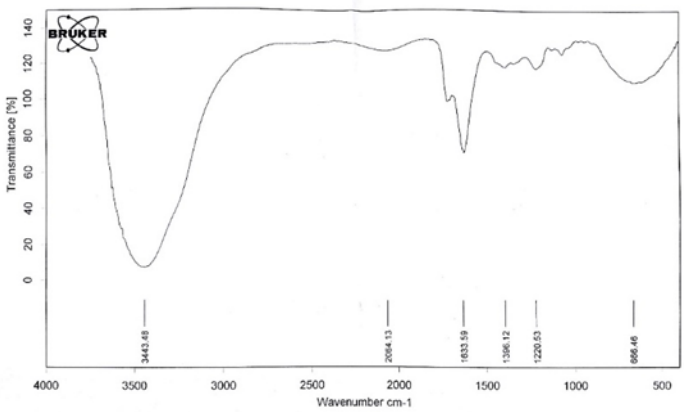

Figure 2: FT-IR spectrum of N-QGDs

XRD analysis

The XRD pattern shown in Figure 3 contains a broad peak centered at 2θ= 21.88° corresponding to an interlayer spacing of the N-GQDs. Such a low diffraction degree suggests a large interlayer spacing, which may be due to the high oxygen content of these N-GQDs, as pointed out by Dong et al [41]. In their study, the interlayer spacing of GQDs increases with the increase in oxygen content.

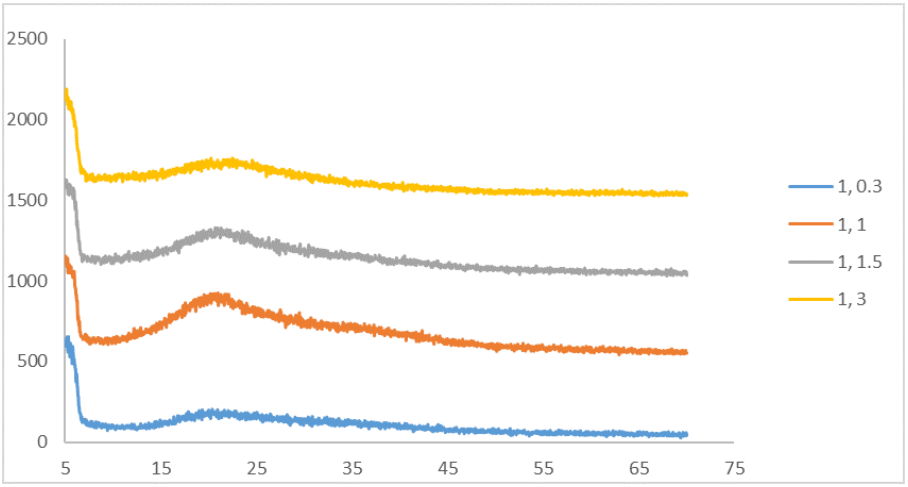

Figure 3: XRD patterns of N-GQDs

TGA

Thermogravimetric analysis (TGA) graphs (Figure. 4) show weight profiles of GQDs variation of temperature (heating rate, 1/min) under N_2 flow. Figure 4a, b (1: 0.3, 1: 1) Weight loss (2.6 wt%) of the GQD up to 100 C could be primarily due to evaporation of water molecules held in the samples [42, 43]. The significant weight loss of 29.59% at 190 °C, presumably due to the loss of

those oxygen-containing groups before the complete oxidative decomposition of the GQD over 268-700 °C. Figure 4c (1: 1.5) Weight loss (3.1 wt%) of the GQD up to 100 C could be primarily due to evaporation of water molecules held in the samples.55-56. The significant weight loss of 22.79% at 190 °C, presumably due to the loss of those oxygen-containing groups before the complete oxidative decomposition of the GQD over 258-700 °C. Figure 4d (1: 3) Weight loss (5.4 wt%) of the GQD up to 100 C could be primarily due to evaporation of water molecules held in the samples.55-56. The significant weight loss of 25.15% at 190 °C, presumably due to the loss of those oxygen-containing groups before the complete oxidative decomposition of the GQD over 249-700 °C.

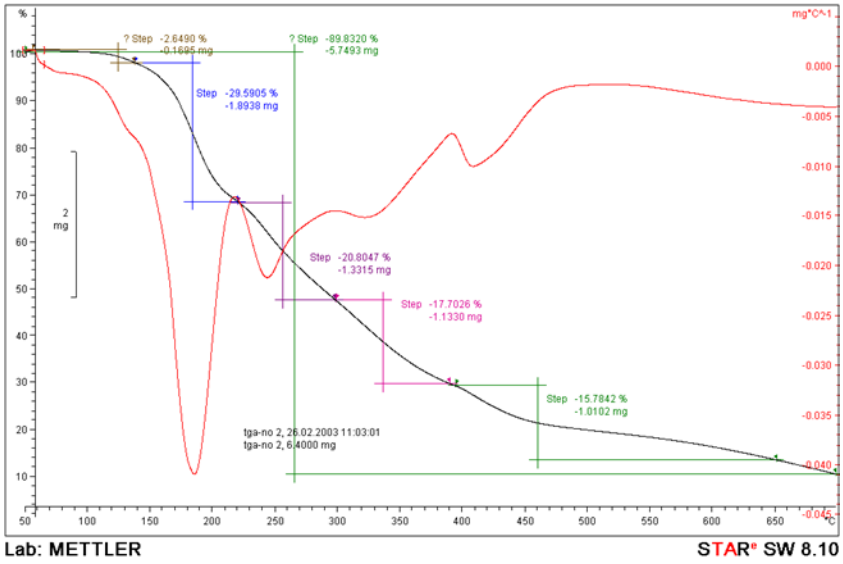

(a)

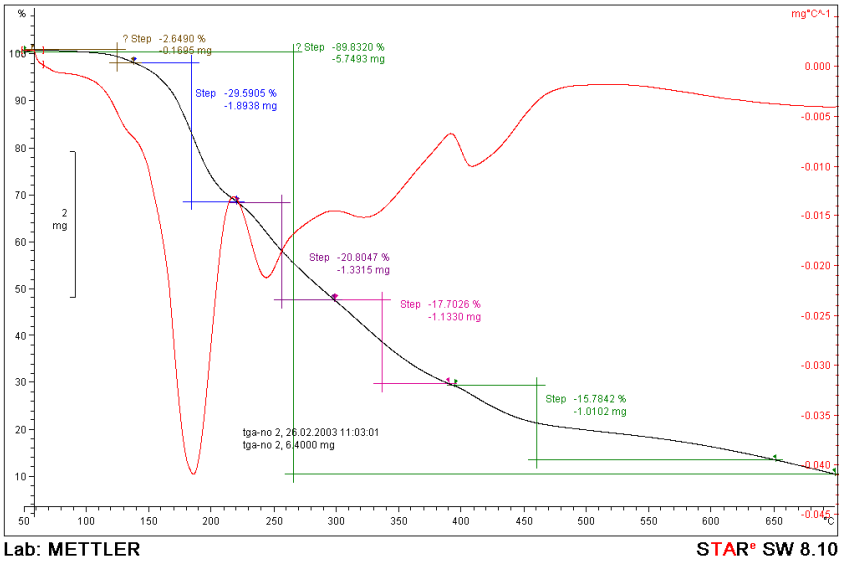
%
mg*C^-1
? Step -2.6490 %
-0.1695 mg
? Step -89.8320 %
-5.7493 mg
Step -29.5905 %
-1.8938 mg
2
mg
Step -20.8047 %
-1.3315 mg
Step -17.7026 %
-1.1330 mg
Step -15.7842 %
-1.0102 mg
tga-no 2, 26.02.2003 11:03:01
tga-no 2, 6.4000 mg
°C
Lab: METTLER
STARe SW 8.10

(b)

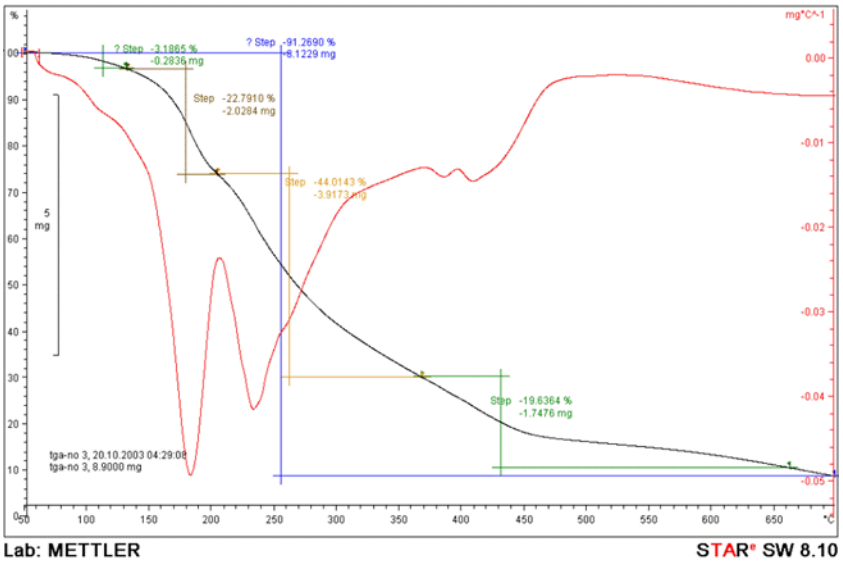
%
mg*C^-1
? Step -3.1865 %
-0.2836 mg
? Step -91.2690 %
-8.1229 mg
Step -22.7910 %
-2.0284 mg
Step -44.0143 %
-3.9173 mg
5
mg
Step -19.6364 %
-1.7476 mg
tga-no 3, 20.10.2003 04:29:08
tga-no 3, 8.9000 mg
°C
Lab: METTLER
STARe SW 8.10

(c)

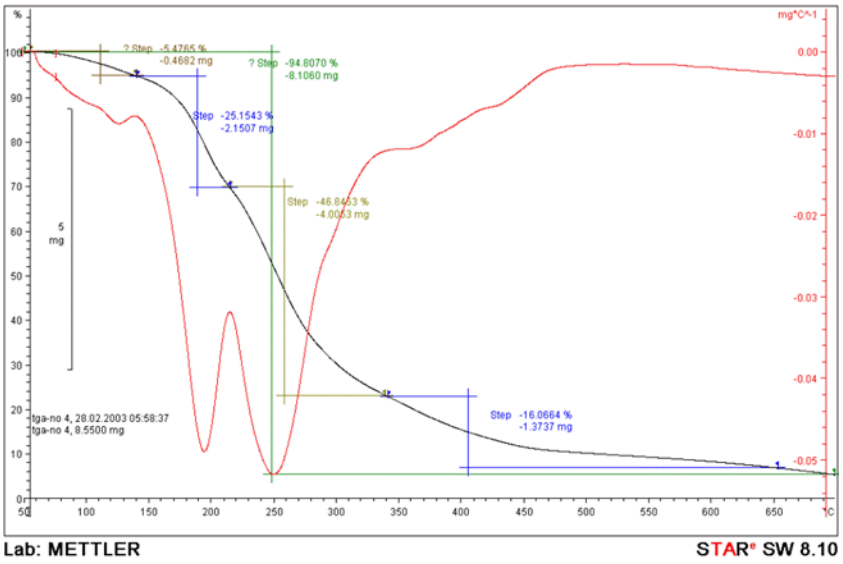

(d)

Figure 4: Thermogravimetric spectrum of GQDs

Photoluminescence analysis

The strong photoluminescence (Fig. 5a) at 383 nm in GQDs is resulted from free zigzag sites with a carbene-like triplet ground state [27]. The initial concentration of DHAA in the hydrothermal treatment can also affect the photoluminescence. By changing the amount of DHAA from ratio of 1: 1 to 1 :3, the intensity of N-GQDs showed drastic decrease, as shown in Fig. 5, indicating the tunable photoluminescence by the control of N-atom ratio. For a detailed PL study of N-GQDs, we carried out PL measurements by using different excitation wavelengths, as shown in Fig. 5. As the excitation wavelength is changed from 200 to 500 nm, each ratio of N-GQDs showed different peaks in three wavelengths (Fig. 5b-e) in which every four ratio exhibited peak at 383 nm, that ratio of 1: 1 has the most intensity.

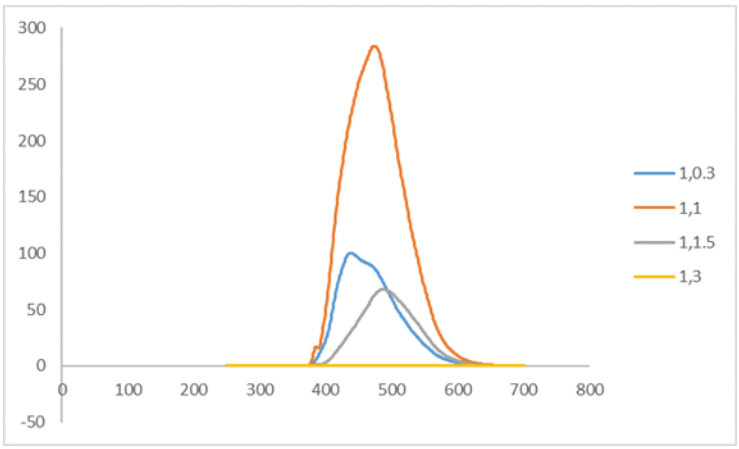

(a)

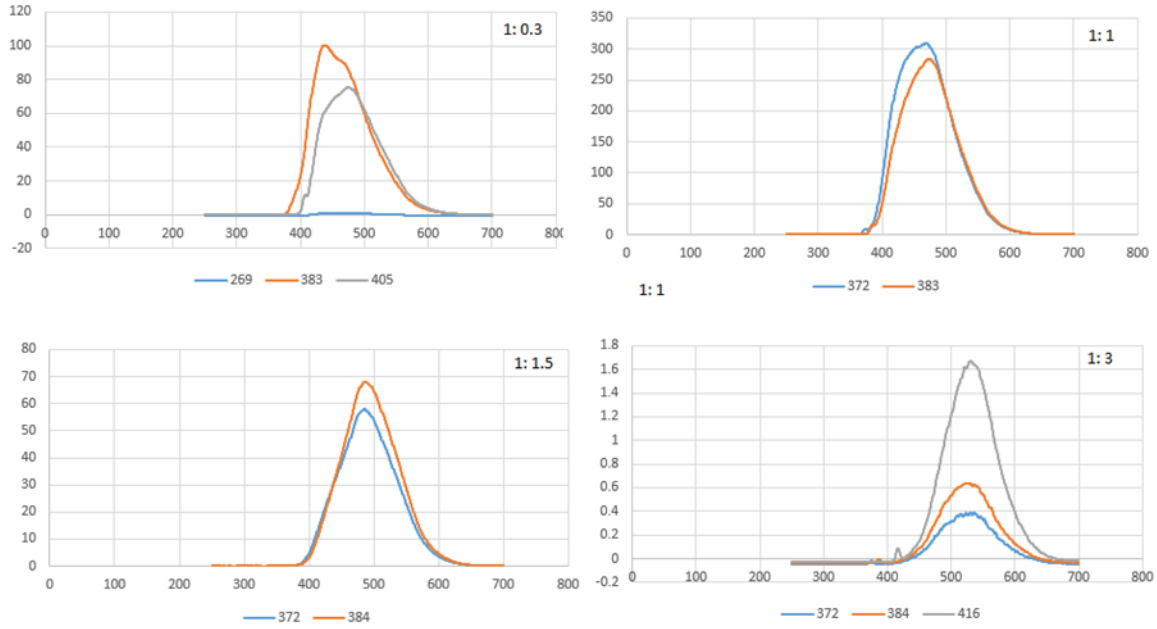

(b)

Figure 5: Fluorescence diagram of N-GQDs

Conclusion

In this study, CA and DHAA with different ratio were reacted together. Considering that DHAA has two active sites, including N and OH, can couple by CA from two positions, this coupling can be occurred as nucleophilic attack of N and water removal by OH groups of two molecules. This process cause's appearance of N-H groups in N-GQDs

which effects on fluorescence and morphology of N-GQDs. Furthermore, up to now most of GQDs are synthesized with CA and ammonia [44]. Because ammonia is a volatile compound during working with it, vigorous and closed system is needed. Despite ammonia, DHAA is a stable material which doesn't requires any isolated system.

The fluorescence emission spectra of GQDs were primarily investigated under excitation wavelengths. From the fluorescence spectra (Fig. 5), GQDs have wonderful emission under excitation wavelength from 300 nm to 400 nm that was similar to previous report.(9) This phenomenon is common and contributed to the surface state affecting the band gap of GQDs. The surface state is analogous to a molecular state whereas the size effect is a result of quantum dimensions, both of which contribute to the complexity of the excited states of GQDs [45]. Particularly, the 52% of quantum yield of the GQDs was calculated at 330 nm optimal excitation according to the above comparative equation. This result is higher when compared with previous report [46, 47].

According to above paragraph our products are quantum dot sized. In contrast to other proportion, 1: 1 ratio has the best florescence effect (280 a.u.). Results showed that florescence effect decreased by increase in molar ratio of DHAA which shows a distinct increase N-GQDs size.

Compared with other proportions of N-QGDs, X-ray diffractogram of 1: 1 ratio has the highest intensity (419 a.u.). Increase in molar ratio of DHAA cause's decrease in XRD intensity. Also, by increasing ratio of DHAA, viscosity of N-GQDs decreased, too. So that the 1: 3 proportion has great fluidity. Color of N-GQDs differ from light yellow to dark brown. Darkening procedure is based on increase in DHAA molar ratio (Figure. 6).

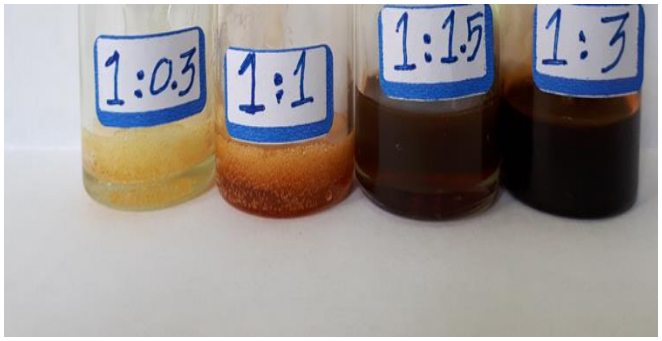

Figure 6: Differing color of N-GQDs

Acknowledgements

This work was supported by the office of the research vice chancellor of Azarbaijan Shahid Madani University.

References

1. Zhang, Z.; Zhang, J.; Chen, N.; Qu, L.; Energy Environ. Sci.. 2012, 5, 8869-90.
2.Shen, J.; Zhu, Y.; Yang, X.; Li, C.; Chem.com. 2012, 48, 3686-99.
3. Liu, WW.; Feng, YQ,; Yan, XB.; Chen, JT.; Xue, QJ.; Adv. Funct. Mater. 2013, 234164.
4. Aillon, KL.; Xie, Y.; El-Gendy, N.; Berkland. CJ.; Forrest, ML.; Adv. Drug Deliv. Rev. 2009, 61, 457-66.
5. Wang, K.; Gao, Z.; Gao, G.; Wo, Y.; Nanoscale Res. Lett. 2013, 8, 122.
6. Zhao, Q-L.; Zhang, Z-L.; Huang, B-H.; Peng, J.; Zhang, M.; Pang, D-W.; Chem.Com. 2008, 41, 5116-8.
7. Zheng, L.; Chi, Y.; Dong, Y.; Lin, J.; Wang, B.; J. Am. Chem. Soc. 2009, 131, 4564-5.
8. Liu, H.; Wang, Q.; Shen, G.; Zhang, C.; Li, C.; Ji, W.; Nanoscale Res. Lett. 2014, 9, 397.
9. Zhu, S.; Meng, Q.; Wang, L.; Zhang, J.; Song, Y.; Jin, H.; Angew. Chem. 2013, 125, 4045-9.
10. Yang, X.; Zhuo, Y.; Zhu, S.; Luo, Y.; Feng, Y.; Dou, Y.; Biosensors and Bioelectronics. 2014, 60, 292-8.
11. Cao, L.; Sahu, S.; Anilkumar, P.; Bunker, CE.; Xu, J.; Fernando, KS.; J. Am. Chem. Soc. 2011, 133, 4754-7.
12. Qu, S.; Wang, X.; Lu, Q.; Liu, X.; Wang, L.; Angew. Chem 2012, 51, 12215-8.
13. Qian, Z.; Ma, J.; Shan, X.; Feng, H.; Shao, L.; Chen, J.; Chem. Eur. J. 2014, 20, 2254-63.
14. Nie, H.; Li, M.; Li, Q.; Liang, S.; Tan, Y.; Sheng, L.; Chem. Mater. 2014, 26, 3104-12.
15. Gude, V.; Beilstein J. Nanotechnol. 2014, 5, 1513.
16. Jiang, C.; Wu, H.; Song, X.; Ma, X.; Wang, J.; Tan, M.; Talanta. 2014, 127, 68-74.
17. Thakur, M.; Pandey ,S.; Mewada, A.; Patil, V.; Khade, M.; Goshi, E.; J. Drug Deliv. 2014.
18. Sun, Y-P.; Zhou, B.; Lin, Y.; Wang, W.; Fernando, KS.; Pathak, P.; J. Am. Chem. Soc.. 2006, 24, 7756-7.
19. Peng, H.; Travas-Sejdic, J.; Chem. Mater. 2009;21, 5563-5.
20. Ma, Z.; Ming, H.; Huang, H.; Liu, Y.; Kang, Z.; New J Chem. 2012, 36, 861-4.
21. Zhang, R.; Chen, W.; Biosensors and Bioelectronics. 2014, 55, 83-90.
22. Guo, Y.; Wang, Z.; Shao, H.; Jiang, X.; Carbon. 2013, 52, 583-9.
23. Fan, R-J.; Sun, Q.; Zhang, L.; Zhang, Y.; Lu, A-H.; Carbon. 2014, 71, 87-93.
24. Zhang, Y-Q.; Ma, D-K.; Zhuang, Y.; Zhang, X.; Chen, W.; Hong, L-L.; J. Mater. Chem. 2012, 22, 16714-8.

25. Liu, Y.; Xiao, N.; Gong, N.; Wang, H.; Shi, X.; Gu, W.; Carbon. 2014,68, 258-64.
26. Shen, J.; Zhu, Y.; Yang, X.; Zong, J.; Zhang, J.; Li, C.; New. J. Chem. 2012, 36, 97-101.
27. Pan, D.; Zhang, J.; Li, Z.; Wu, M.; Adv. mater. 2010, 22, 734-8.
28. Shen, J.; Zhu, Y.; Chen, C.; Yang, X.; Li, C.; Chem. Com. 2011, 47, 2580-2.
29. Yan, X.; Cui, X.; Li, B.; Li, L-s.; Nano let. 2010, 5, 869-73.
30. Liu, R.; Wu, D.; Feng, X.; Müllen, K.; Journal of the American Chemical Society. 2011, 133, 15221-3.
31. Liu, H.; Liu, Y.; Zhu, D.; J. Mater. Chem. 2011, 21, 3335-45.
32. Li, Y.; Zhou, Z.; Shen, P.; Chen, Z.; S Acs Nano. 2009, 3,1952-8.
33. Li, Q.; Zhang, S.; Dai, L.; Li, L-s.; J. Am. Chem. Soc. 2012, 134, 18932-5.
34. Hu, C.; Liu, Y.; Yang, Y.; Cui, J.; Huang, Z.; Wang, Y.; J. Mater. Chem. B. 2013, 1, 39-42.
35. Derycke, V.; Martel, R.; Appenzeller, J.; Avouris, P.; Appl. Phys. Lett. 2002, 80, 2773-5.
36. Gong, K.; Du ,F.; Xia, Z.; Durstock, M.; Dai, L.; Sci. 2009, 323760-4.
37. Wang, S.; Wang, X.; Jiang, SP.; J. A. Sci. 2008, 24, 10505-12.
38. Wang, S.; Yang, F.; Jiang, SP.; Chen, S.; Wang, X.; Electrochem. Com. 2010, 12, 1646-9.
39. Zhou, C.; Kong, J.; Yenilmez, E.; Dai, H.; Sci. 2000, 290, 1552-5.
40. Wang, Y.; Shao, Y.; Matson, DW.; Li, J.; Lin, Y.; ACS nano. 2010, 4, 1790-8.
41. Dong, Y.; Chen, C.; Zheng, X..; Gao, L.; Cui, Z.; Yang, H.; J. Mater. Chem. 2012, 22, 8764-6.
42. Stankovich, S.; Dikin, DA.; Piner, RD.; Kohlhaas, KA.; Kleinhammes, A.; Jia ,Y.; Carbon. 2007, 45, 15, 1558-65.
43. Park, S.; An, J.; Piner, RD.; Jung, I.; Yang, D.; Velamakanni, A.; Chem. mater. 2008, 20, 6592-4.
44. Van Tam, T.; Trung, NB.; Kim, HR.; Chung, JS.; Choi, WM;. Sensors and Actuators B: Chemical. 2014, 202, 568-73.
45. Shang, J.; Ma, L.; Li, J.; Ai, W, Yu. T.; Gurzadyan, GG.; Sci. Rep. 2012, 2, 792.
46. Sun, W.; Du, Y.; Wang, Y.; J. Lumin. 2010, 130, 1463-9.
47. Du, F.; Zeng, F.; Ming, Y.; Wu, S.; Mikrochim. Acta. 2013, 180, 453-60.